DOI: 10.1002/ejic.200700790

Synthesis, X-ray Crystal Structures and Electrochemistry of (Indenyl)-ruthenium Complexes Containing dppf and Heterocyclic Thiolato/Thione Ligands

Sin Yee Ng,[a] Weng Kee Leong,[a] and Lai Yoong Goh,*[a][‡] and Richard D. Webster*[b]

Keywords: Cyclic voltammetry / Electron localization / Ruthenium / Heterocyclic thiolates/thiones / X-ray crystal structures

A number of (indenyl)ruthenium complexes containing dppf [1,1′-bis(diphenylphosphanyl)ferrocene] and heterocyclic thiolato/thione ligands have been synthesized. All the complexes were fully characterized by microanalytical and spectroscopic techniques, together with X-ray diffraction analyses for those containing the benzothiazolato (thiolato) and the thiadiazole (thione) ligands. Cyclic voltammetry (CV) experiments indicated that these complexes can be oxidized in three one-electron processes at positive potentials. Differences in chemical reversibility observed during variable-temperature CV experiments indicated that it was likely that the oxidation processes occurred at two electronically non-communicating sites within the molecules. One site could be assigned as the oxidation of the Ru ion (two one-electron processes), whilst the second site was assigned as the oxidation of the dppf (one one-electron process).

Introduction

There exists continuing interest in (N,S-) heterocyclic thiolato ligands on account of their presence in many bioactive molecules.[1] Containing both an endocyclic hard donor N atom and an exocyclic soft donor S atom, the derivative thiolato ligands, which belong to a class of heterocyclic thionates, form metal complexes possessing both biomedical and industrial applications.[2] An additional feature of these compounds is their tendency to undergo tautomerization in solution to thione,[2a,3] which is the dominant form in polar solvents and in the solid state. It is of interest to examine the underlying cause for the preferred form of the ligand upon coordination. This study was prompted by the scarcity in the literature of half-sandwich Ru complexes containing heterocyclic ligands. To the best of our knowledge, there is only one reported example, [$CpRu(PPh_3)_2$-(heterocyclic thiolato)], where "heterocyclic thiolato" stands for the 2-mercaptobenzimidazolato (**A**), 2-mercaptobenzothiazolato (**B**), and 2-mercaptobenzoxazolato (**C**) ligands, as shown in Figure 1.[4]

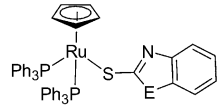

E = NH (**A**); S (**B**); O (**C**)

Figure 1. Heterocyclic thiolato complexes of CpRu.

In previous work on indenyl (or arene, Cp or Cp*) ruthenium complexes, we examined the electrochemical behavior and lability of the indenyl and chlorido ligands of [RuCl(dppf)(ind)] (**1**) and the related [RuCl(dppm)(ind)] complex [dppm = bis(diphenylphosphanyl)methane] in their reactions with selected donor ligands L, viz. phosphane,[5] monothiolato[6] and dithiolato ligands.[7] We found that most of the [Ru(dppf)(ind)(L)] compounds underwent two or three one-electron oxidation processes, and we proposed that the oxidation processes occurred at different localized (noncommunicating) sites within the molecules. The two proposed localized sites of oxidation were based on observations of how the oxidation potentials shifted as the Ind (or other aromatic ligands), or L groups were systematically varied. In this work, the nature of the L groups has been extended to heterocyclic thiolato and thione ligands to enable a more detailed electrochemical investigation (Figure 2). The degree of electron delocalization following oxidation is often difficult to assess in unsymmetrical molecules, because of the uncertainty in the position of electron transfer.[8] In symmetrical compounds, the level of communication is often determined by electrochemical and UV/Vis spectroscopic experiments.[9]

[a] Department of Chemistry, National University of Singapore, 3 Science Drive 3, Singapore 117543
E-mail: laiyoonggoh@ntu.edu.sg
[b] Division of Chemistry and Biological Chemistry, School of Physical and Mathematical Sciences, Nanyang Technological University,
Singapore 637371, Singapore
E-mail: webster@ntu.edu.sg
[‡] Current address: Division of Chemistry and Biological Chemistry, School of Physical and Mathematical Sciences, Nanyang Technological University,
Singapore 637371, Singapore

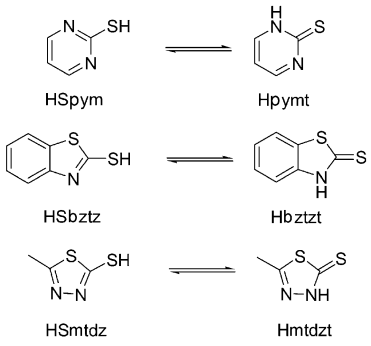

Figure 2. Some heterocyclic thiol/thione tautomers.

Results and Discussion

Synthesis and Reactivity

The ambient temperature reactions of **1** with 1.1–1.5 molar equivalents of the heterocyclic thiols 2-mercaptopyrimidine (HSpym), 2-mercaptobenzothiazole (HSbztz) and 2-mercapto-5-methyl-1,3,4-thiadiazole (HSmtdz) yielded the products shown in Scheme 1. The reaction with HSpym in MeOH, (route a), with or without $NaBPh_4$ as a Cl^- abstractor, resulted in the displacement of the Ind ligand to yield [Ru(dppf)$(Spym)_2$] (**3**) as yellow crystals in 37% yield, with 36% recovery of **1**. The formation of bis(Spym) complex **3**, despite the use of only 1.1 molar equivalents of HSpym with respect to **1**, is indicative of an efficient labilizing effect on Ind. A similar result was obtained when the reaction was repeated in CH_2Cl_2. We had reported a precedence for similar labilizing of the Ind ligand in the reaction of **1** with dialkyl dithiocarbamates and observed that the lability of Ind depends on the incoming dithiolato ligand and the nature of the solvent medium.[7] In this context, we point out that our earlier reaction of [RuClCp(dppf)] with pyridine-2-thiol in the presence of $NaBPh_4$ resulted only in chlorido substitution to afford the ionic complex, [RuCp(dppf)(pySH)]BPh_4 (D) (where pySH = pyridine-2-thione), arising from thiol/thione tautomerization of pyridine-2-thiol. (Scheme 2).[10] The reaction with HSbztz, (route b) resulted in Cl^- displacement, giving [Ru(dppf)(ind)(Sbztz)] (**4**) in 60% yield, with no byproduct indicative of Ind ligand dissociation. With HSmtdz, the reaction yielded an ionic product, [Ru(dppf)(Hmtdzt)(ind)]Cl [**5**]Cl (route c). The coordination of the heterocyclic ligand as a thione is supported by IR spectroscopic evidence for the presence of the NH stretch and an X-ray diffraction analysis (see below). This observed thione coordination indicates a rapid thiol/thione tautomerization of HSmtdz, in favor of thione, in solution, in agreement with reported spectroscopic studies and computational calculations.[3a] Indeed, a small amount of tautomerized HSmtdz was isolated from the product mixture. However, if the reaction is repeated in the presence of $NaBPh_4$ (which acts as a halide abstractor), an uncharged species, [Ru(dppf)(ind)(Smtdz)] (**5a**), was isolated (route d). The formulation of **5a** was supported by spectroscopic and microanalytical data. Consistent with its neutrality is its high solubility in nonpolar solvents, like benzene or toluene.

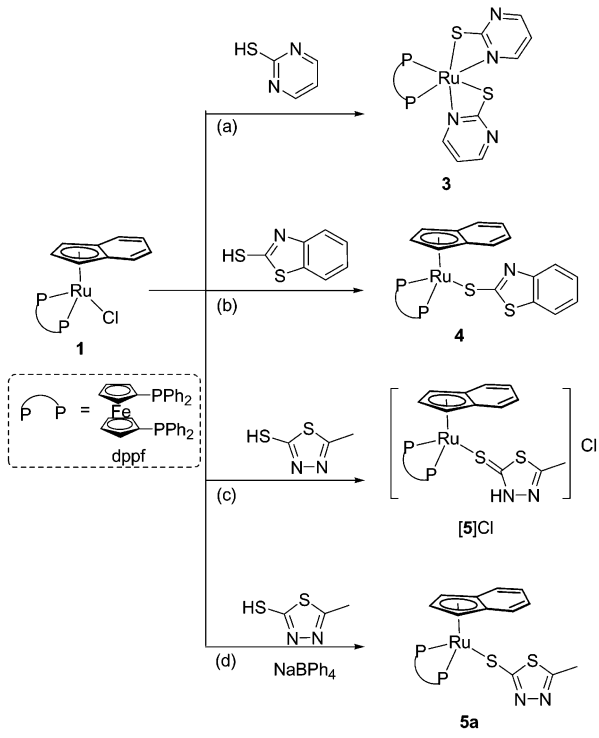

Scheme 1.

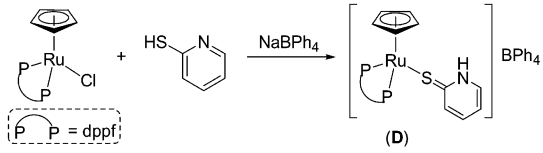

Scheme 2.

The reactions of [Ru(CH_3CN)(dppf)(ind)]PF_6 ([**2**]PF_6) with heterocyclic ligands led to the formation of ionic thione-coordinated derivatives, viz. [Ru(dppf)(Hmtdzt)(ind)]PF_6 ([**5**]PF_6), [Ru(dppf)(Hpymt)(ind)]PF_6 ([**6**]PF_6), and [Ru(dppf)(Hbztzt)(ind)]PF_6 ([**7**]PF_6), in high yields (Scheme 3). Thione coordination is supported by the presence of NH stretches in their IR spectra, and the presence of η^5-Ind is clearly evident in the ^1H NMR spectra (see Experimental Section). These complexes were found to be unstable in solution, with a stability order of $\mathbf{5}^+ > \mathbf{7}^+ > \mathbf{6}^+$. In CH_3CN, all three salt species undergo thione displacement by the solvent within minutes, a conversion readily shown by a gradual color change from red to yellow. However, this conversion can be reversed by the addition of ether, with crystallization of their original PF_6 salts, which is indicative of a reversible equilibrium in CH_3CN. In the presence of $[(Ph_3P)_2N]Cl$ {bis(triphenylphosphane)iminium chloride, [PPN]Cl}, the coordinated thione in complex [**7**]-PF_6 can be displaced, resulting in reversion to the chlorido

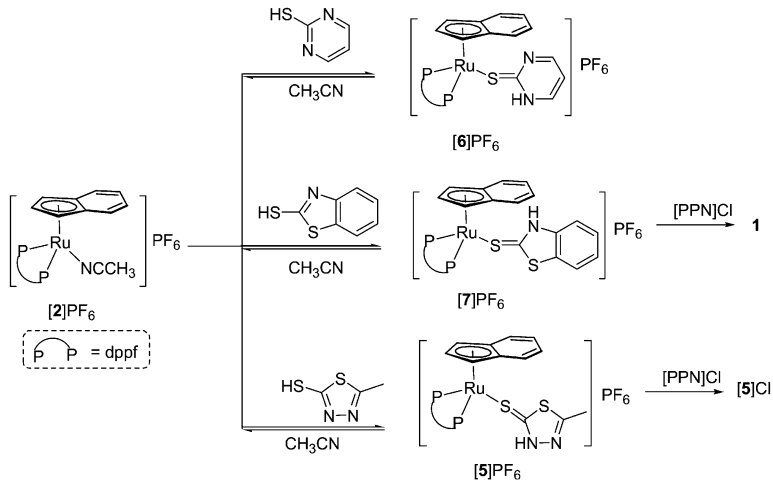

Scheme 3.

complex **1**. In comparison, the thione ligand in complex [**5**]-PF_6 is firmly bound, and the complex only undergoes anion exchange in the presence of [PPN]Cl. Stable in thf, complex [**6**]PF_6 decomposes quickly at room temperature in CH_2Cl_2 and acetone, giving green and dark brown solutions, respectively. However, [**6**]PF_6 is sufficiently stable below –20 °C in CH_2Cl_2 for cyclic voltammetry experiments to be performed (see below).

Crystallographic Studies

Complexes **4** and [**5**]Cl have been studied by X-ray diffraction analyses and their ORTEP diagrams are shown in Figure 3 and Figure 4, respectively. Selected bond parameters are given in Table 1 and crystal refinement data in Table 2.

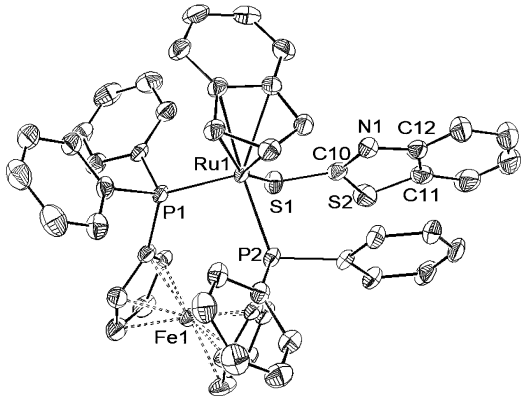

Figure 3. ORTEP diagram of **4**. Thermal ellipsoids are drawn to 50% probability level. Hydrogen atoms are omitted for clarity.

The geometry around the Ru centers in both **4** and [**5**]Cl is distorted octahedral; the capping indenyl ligand occupies the three facial sites, while chelating dppf and S1 of the monodentate heterocyclic ligand reside on the other three sites. The indenyl ligands on both complexes show slight $\eta^5 \rightarrow \eta^3$ distortion, as commonly observed.[11]

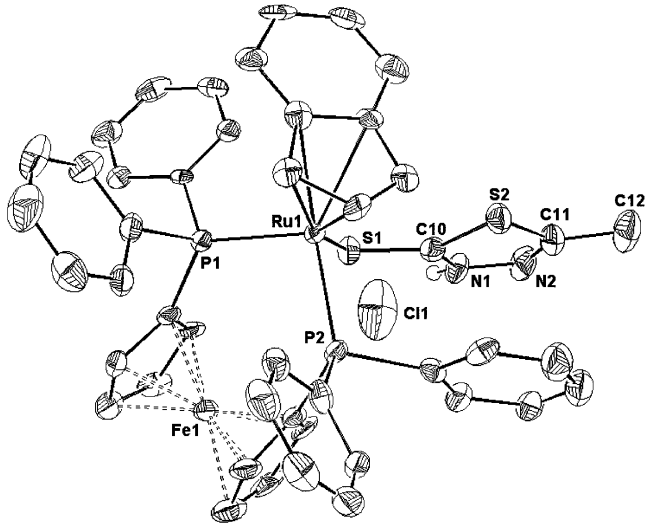

Figure 4. ORTEP diagram of [**5**]Cl. Thermal ellipsoids are drawn to 50% probability level. Hydrogen atoms are omitted for clarity.

In complex **4**, the Ru1–S1 distance [2.4086(9) Å] is in the normal range for the Ru–S bond length.[10,12,13] The long N1–Ru1 distance (3.676 Å) is clearly indicative of the absence of any interaction between the two atoms [cf. N–Ru 2.242(6) Å for the bidentate Sbztz ligand].[12] The short N1–C10 bond length [1.295(5) Å] indicates double-bond character, while the longer N1–C12 bond [1.388(5) Å] is a single bond. The bond angles of the heterocyclic ligand are comparable to those found in other monodentate Sbztz ligands.[13a] The metric data of the coordinated Hmtdzt thione moiety in [**5**]Cl is in close agreement with those of the free Hmtdzt molecule.[3a] However, due to the coordination of S1 to Ru1, the electron density around S1–C10 bond is remarkably reduced, resulting in a longer bond length of 1.703(11) Å [cf. 1.6690(13) Å in free thione].[3a] Noticeable is the substantially shorter C10–S2 bond in [**5**]Cl, when compared with that in **4**, which is close to the corresponding bond lengths [1.659(4)–1.695(7) Å] observed for other thione-coordinated Ru complexes.[10]

Table 1. Slip-fold parameters,[a] selected bond lengths [Å] and angles [°].

Complexes	**4**·2C_4H_8O	[**5**]Cl·CH_2Cl_2·H_2O
Δ [Å]	0.168	0.174
Hinge angle (HA) [°]	7.06	6.62
Fold angle (FA) [°]	10.77	10.34
C*–Ru1	1.920	1.923
Ru1–P1	2.3133(9)	2.331 (3)
Ru1–P2	2.2666 (9)	2.273 (3)
Ru1–S1	2.4086 (9)	2.397 (3)
S1–C10	1.729 (4)	1.703 (11)
C10–S2	1.783 (4)	1.727 (11)
C10–N1	1.295 (5)	1.325 (13)
S2–C11	1.735 (5)	1.731 (11)
N2–C11	–	1.280 (15)
N1–N2	–	1.373 (12)
N1–C12	1.388 (5)	–
C11–C12	1.396 (6)	1.489 (16)
P1–Ru1–P2	98.50 (3)	98.47 (10)
P1–Ru1–S1	88.10 (3)	86.10 (9)
P2–Ru1–S1	86.88 (3)	86.47 (10)
Ru1–S1–C10	110.59 (13)	114.3 (4)
S1–C10–S2	115.1 (2)	128.5 (6)
S1–C10–N1	130.3 (3)	122.6 (8)
S2–C10–N1	114.6 (3)	108.8 (8)
C10–S2–C11	89.1 (2)	88.9 (5)
C10–N1–C12	111.1 (3)	–
C10–N1–N2	–	117.4 (10)
N1–N2–C11	–	110.0 (9)
N2–C11–S2	–	114.8 (8)

[a] Δ: the difference in the average bond lengths of the metal to the ring junction carbons, i.e. C4, C9, and of the metal to adjacent carbon atoms of the five-membered ring, i.e. C1, C3. HA: angle between the planes defined by [C1,C2,C3] and [C1,C3,C4,C9]. FA: angle between the planes defined by [C1,C2,C3] and [C4,C5,C6,C7,C8,C9].[11] (See Figure 6 for atom numbering codes.) C*: centroid of C1, C2, C3, C4 and C9.

Electrochemical Studies

The cyclic voltammograms obtained in CH_2Cl_2 solutions containing **4**, **5a**, and [**5**–**7**]PF_6 at two different temperatures are displayed in Figure 5. Each compound displayed three oxidation processes, with similar peak current values indicating that the processes occurred by the same number of electrons (i.e. n = 1). Closely related compounds containing an indenyl (or arene, Cp or Cp*) and a dppf (or similar phosphanyl) group also often display two or three one-electron oxidation processes.[14]

Interestingly, for most of the compounds the anodic (i_p^{ox}) to cathodic (i_p^{red}) peak current ratio (i_p^{ox}/i_p^{red}) for the second process became closer to unity as the temperature was raised. Normally, in cases of chemical instability of oxidized compounds, the i_p^{ox}/i_p^{red} value becomes closer to unity as the temperature is lowered, because of improved stability of the reactive species. Therefore, the apparent reverse trend with temperature for the second oxidation process may be due to a follow-up chemical equilibrium reaction (such as a structural change) that is slowed down at higher temperatures.

Data from cyclic voltammograms suggest that the first and third oxidation processes are closely related, while the second process occurs essentially independently of the first and third processes. This is demonstrated by the experiments at low temperature, where the first and third processes have i_p^{ox}/i_p^{red} values close to one, whilst the second process appears chemically irreversible (since it is not normal to detect a chemically reversible electron-transfer process at a potential greater than that for an apparently chemically irreversible process).

Table 2. Crystal and refinement data.

	4·2C_4H_8O	[**5**]Cl·CH_2Cl_2·H_2O
Formula	$C_{58}H_{55}FeNO_2P_2RuS_2$	$C_{47}H_{43}Cl_3FeN_2OP_2RuS_2$
Molecular weight	1081.01	1041.16
Space group (crystal system)	$P\bar{1}$	$P2_1/n$
Crystal system	triclinic	monoclinic
a [Å]	12.1349 (15)	11.5588 (4)
b [Å]	12.3110 (16)	15.0780 (6)
c [Å]	16.970 (2)	25.8460 (11)
α [°]	77.510 (2)	90
β [°]	78.613 (2)	93.444 (2)
γ [°]	87.454 (2)	90
Cell volume [Å^3]	2426.5 (5)	4496.4 (3)
Z	2	4
$D_{calcd.}$ [g cm^{-3}]	1.480	1.538
Absorption coefficient [mm^{-1}]	0.808	1.040
F(000) electrons	1116	2120
Crystal size [mm]	0.36 × 0.20 × 0.10	0.14 × 0.04 × 0.04
θ range for data collection [°]	1.25–27.50	1.56–24.00
Index ranges	$-15 \le h \le 15$	$-13 \le h \le 13$
	$-15 \le k \le 15$	$-17 \le k \le 13$
	$-22 \le l \le 22$	$-29 \le l \le 29$
Reflections collected	30448	23703
Independent reflections	11092	7068
Max. and min. transmission	0.9236–0.7597	0.9596–0.8681
Data/restraints/parameters	11092/38/604	7068/3/537

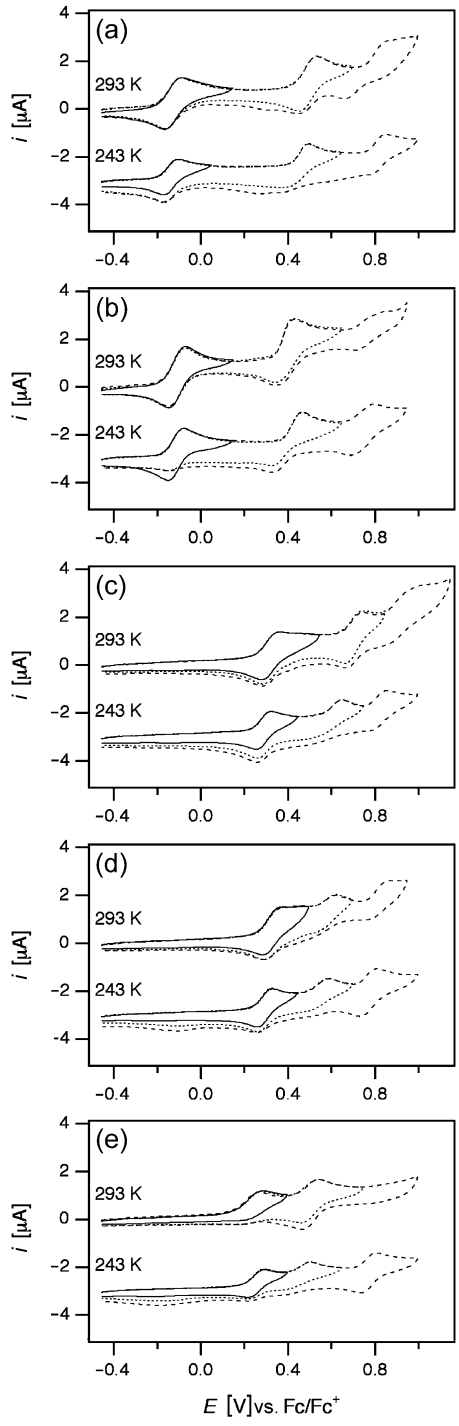

Figure 5. Cyclic voltammograms recorded at 100 mV s^{-1} at a 1-mm planar GC electrode in CH_2Cl_2 with 0.25 M Bu_4NPF_6. (a) 0.77 mM [**4**]. (b) 1.07 mM [**5a**]. (c) 0.85 mM [**7**]PF_6. (d) 0.81 mM [**5**]PF_6. (e) 0.74 mM [**6**]PF_6. Voltammograms at 243 K are offset by –3 μA.

The CV data obtained for [**6**]PF_6 were particularly interesting and unusual [Figure 5(e)]. At 243 K, the first (least positive) and third (most positive) processes for solutions of [**6**]PF_6 appear chemically reversible, but at 293 K, where the first process appears chemically irreversible, the third process is not detected (but the second process appears to be chemically reversible). The lack of the third (most positive) process at 293 K in solutions of [**6**]PF_6 is consistent with the decomposition of the moiety responsible for the first process, but the section of the molecule responsible for the second process remains largely intact.

One explanation consistent with the voltammetric data is that the first and third processes are associated with the oxidation of the Ru^{II} ion (to Ru^{III} and then to Ru^{IV}), while the second process is associated with oxidation in the vicinity of dppf. Under these conditions, it is possible for the chemical reversibility of the second process to appear to be independent of the first and third processes, implying that the two separate oxidation sites are noncommunicating. Free dppf is oxidized at an approximately +200 mV more positive potential than ferrocene.[15] The oxidation occurs by one-electron, but the product is not as stable as the Fc/Fc^+ system, and moderate scan rates of around 3 V s^{-1} are needed to obtain i_p^{ox}/i_p^{red} ratios equal to unity.[15] When dppf is coordinated to other metal ions through the phosphorus atoms, the oxidation potential increases to approximately +0.5 V vs. Fc/Fc^+, and the stability of the oxidized dppf is substantially improved so that i_p^{ox}/i_p^{red} ratios equal to unity are obtained at slow scan rates of 100 mV s^{-1} (similar to Fc/Fc^+).[15,16] In this work, the second oxidation process occurs at approximately 0.4–0.7 V vs. Fc/Fc^+ (Table 3), a value similar to that expected for coordinated dppf. The conclusion that the first process is associated with oxidation in the region of the Ru ion is consistent with the observation that the first oxidation potential is similar for **4** and **5a** (ca. –0.1 V vs. Fc/Fc^+) and similar for [**5**]PF_6, [**6**]PF_6, and [**7**]PF_6 (ca. +0.3 V vs. Fc/Fc^+) (Figure 5 and Table 3), since the potential is likely to be sensitive to the bonding mode of the sulfur atom that is coordinated directly to the ruthenium center.

Table 3. Cyclic voltammetric data obtained at a scan rate of 100 mV s^{-1} with a GC electrode of 1 mm diameter at 243 K or 293 K in CH_2Cl_2 with 0.25 M Bu_4NPF_6 as the supporting electrolyte.

Compound	T [K]	Oxidation Processes[a]			
		E_p^{ox} [V] [b]	E_p^{red} [V] [c]	$E^r_{1/2}$ [V] [d]	ΔE [mV] [e]
4	293	–0.088	–0.166	–0.13	78
	293	+0.533	+0.451	+0.49	82
	243	+0.848			
5a	243	–0.080	–0.149	–0.12	69
	243	+0.465	+0.324	+0.39	141
	243	+0.794	+0.688	+0.74	106
[**5**]PF_6	243	+0.328	+0.257	+0.29	71
	243	+0.584			
	243	+0.806	+0.734	+0.77	72
[**6**]PF_6	243	+0.291	+0.216	+0.25	75
	293	+0.540	+0.460	+0.50	80
	243	+0.804	+0.733	+0.77	71
[**7**]PF_6	243	+0.324	+0.253	+0.29	71
	293	+0.748	+0.662	+0.71	86
	243	+0.854			

[a] All potentials are relative to the ferrocene/ferrocenium redox couple. [b] E_p^{ox}: oxidative peak potential. [c] E_p^{red}: reductive peak potential. [d] $E^r_{1/2} = (E_p^{ox} + E_p^{red})/2$. [e] $\Delta E = |E_p^{ox} - E_p^{red}|$.

Conclusion

The outcome of the substitution of the chlorido ligand of **1** with heterocyclic thiols was found to be highly dependent on the intrinsic chelating tendency of the resulting thiolates and the relative stability of the thiolato/thione complexes. Thus, (i) the indenyl ligand was displaced to give a six-coordinate complex, [Ru(dppf)(Spym)$_2$] (**3**), containing bis(chelating) Spym; (ii) a neutral thiolato complex, [Ru(dppf)(ind)(Sbztz)] (**4**), was isolated from a reaction with HSbztz; (iii) the reaction with HSmtdz gave a thione-coordinated complex, [Ru(dppf)(Hmtdzt)(ind)]Cl [**5**]Cl, as a result of the tautomerization of HSmtdz, while the same reaction in the presence of $NaBPh_4$ as a chloride abstractor, led to the isolation of a neutral complex, [Ru(dppf)(ind)(Smtdz)] (**5a**). The reactions of the solvento complex, [Ru(CH_3CN)(dppf)(ind)]PF_6 ([**2**]PF_6), with the selected heterocyclic thiols all yielded thione-coordinated complexes of [Ru(dppf)(ind)]. These complexes are substitutionally labile, the weakly bound thione ligands being easily displaced by coordinating solvent, i.e. CH_3CN, with reversal to [**2**]PF_6. Cyclic voltammetry experiments indicated that compounds **4**, **5a**, [**5**]$^+$, [**6**]$^+$, and [**7**]$^+$ could be oxidized in three one-electron steps at positive potentials. The results support the hypothesis that the oxidation processes occurs at two independent (noncommunicating) sites within the molecules, most likely at the two metal ions (Ru and Fe).

Experimental Section

General Remarks

All reactions were carried out by using conventional Schlenk techniques under an inert atmosphere of nitrogen or under argon in an M. Braun Labmaster 130 Inert Gas System.

NMR spectra were measured with a Bruker 300 FT NMR spectrometer; for ^{1}H and ^{31}P spectra, chemical shifts were referenced to residual protiated solvent in the deuterio-solvents [C_6D_6, $CDCl_3$, $(CD_3)_2CO$ or C_4D_8O and to external H_3PO_4, respectively]. IR spectra in KBr pellets were measured in the range 4000–400 cm^{-1} by means of a BioRad FTS-165 FTIR instrument. Mass spectra were run with a Finnigan Mat 95XL-T (FAB) or a Finnigan-MAT LCQ (ESI) spectrometer. Elemental analyses were performed by the microanalytical laboratory in-house.

Voltammetric experiments were conducted with a computer-controlled Eco Chemie μAutolab III potentiostat with a glassy carbon working electrode of 1 mm diameter. Potentials were referenced to the ferrocene/ferrocenium (Fc/Fc^+) redox couple, which was used as an internal standard. The electrochemical cell was jacketed in a glass sleeve and cooled between 243–293 K by using a Lauda RL6 variable-temperature methanol-circulating bath.

[RuCl(dppf)(ind)] (**1**) and [Ru(CH_3CN)(dppf)(ind)]PF_6 ([**2**]PF_6) were prepared by published methods.[5] All other chemicals were obtained commercially and used without any further purification. All solvents were dried with sodium/benzophenone and distilled before use. Celite (Fluka AG) and silica gel (Merck Kieselgel 60, 230–400 Mesh) were dried at 140 °C overnight before chromatographic use.

Conventional numbering of indenyl protons shown in Figure 6 is followed in the assignment of NMR signals.

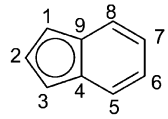

Figure 6. Atom-numbering system for the indenyl ligand.

Reactions of [RuCl(dppf)(ind)] (1)

With HSpym: HSpym (8 mg, 0.07 mmol) was added into a red suspension of **1** (50 mg, 0.062 mmol) in MeOH (10 mL), and the mixture was stirred at room temp. The red suspension slowly turned brownish-red as the reaction proceeded. After 18 h, the resultant brownish-red suspension was evacuated to dryness, and the residue was extracted with a toluene/thf (4:1) mixture (2 × 5 mL). The extract was concentrated to ca. 2 mL and then loaded onto a silica gel column (2 × 8 cm) prepared in *n*-hexane. Elution gave two fractions: (i) an orange-red eluate in toluene/ether (4:1, ca. 10 mL), which gave unreacted **1** (18 mg, 36% recovery); (ii) a yellow eluate in thf (ca. 20 mL), which, upon recrystallization in thf/hexane (1:1), gave yellow solids of [Ru(dppf)(Spym)$_2$] (**3**) (20 mg, 37% yield).

The ^{1}H and ^{31}P NMR spectra of the crude product from a similar reaction in CH_2Cl_2 showed a 1:1 molar mixture of **3** and unreacted **1**.

With HSbztz: A similar reaction with HSbztz (16 mg, 0.096 mmol) gave a red product solution. Chromatography of the extract in toluene yielded two fractions: (i) an orange-red eluate in toluene/thf (2:1, ca. 8 mL), which gave unreacted **1** (6 mg, 12% recovery); (ii) a red eluate in thf/MeOH (4:1, ca. 20 mL), which, upon recrystallization in thf/hexane (1:1), gave red star-shaped crystals of [Ru(dppf)(ind)(Sbztz)] (**4**) (35 mg, 60% yield). X-ray-diffraction-quality single crystals were obtained from a concentrated thf solution of **4**, layered by hexane, after 2 d at –30 °C.

With HSmtdz: (a) In the absence of $NaBPh_4$, a similar reaction with HSmtdz (10 mg, 0.096 mmol) produced a red product solution, which was adsorbed on silica gel. A similar chromatographic workup gave three fractions: (i) a yellow eluate in toluene/ether (10:1, ca. 2 mL), which gave Hmtdzt (tautomerized HSmtdz) upon crystallization, identified by its single-crystal structure that matched the literature report.[17] (2 mg); (ii) a red eluate in toluene/ether (4:1, ca. 3 mL), which gave unreacted **1** (2 mg, 4% recovery); (iii) a red eluate in thf (ca. 8 mL), which gave [Ru(dppf)(Hmtdzt)(ind)]Cl ([**5**]Cl) as red solids (39 mg, 67% yield). Single crystals suitable for X-ray diffraction analysis were obtained from a concentrated solution in CH_2Cl_2, layered with hexane after 5 d at –30 °C.

(b) A similar reaction in the presence of $NaBPh_4$ (32 mg, 0.094 mmol) gave a resultant red solution. A workup as in the reaction with HSbztz yielded two fractions: (i) a red eluate in toluene/thf (2:1, ca. 15 mL), which, upon recrystallization in thf/hexane, gave [Ru(dppf)(ind)(Smtdz)] (**5a**) as red solids (39 mg, 70% yield); (ii) an orange-red eluate in thf (ca. 5 mL), which gave unreacted **1** (3 mg, 6% recovery).

Data

3: ^{1}H NMR (C_6D_6): δ = 3.92–3.94 (m, 4 H, C_5H_4), 4.60, 4.86 (each s, 2 H, C_5H_4), 5.41 (t, $^3J_{HH}$ = 4.95 Hz, 2 H, Spym), 6.91–6.92, 7.00–7.03, 7.11–7.30, 7.61–7.63 and 7.74–7.79 (each m, 24 H, Ph and Spym) ppm. ^{31}P{^{1}H} NMR (C_6D_6): δ = 51.8 (s, dppf) ppm. IR (KBr): $\tilde{\nu}$ = 3049 (w), 2924 (w), 1652 (w), 1558 (m), 1430 (w), 1372 (s), 1248 (w), 1162 (w, CS), 1089 (w), 700 (m), 520 (w) cm^{-1}. FAB$^+$-MS: *m*/*z* = 878 [M + H]$^+$, 767 [M – Spym]$^+$.

$C_{42}H_{34}FeN_4P_2RuS_2$ (877.74): calcd. C 57.5, H 3.9, N 6.4, S 7.3; found C 57.8, H 3.7, N 6.3, S 7.3.

4: ^{1}H NMR (C_6D_6): δ = 3.62, 3.86, 4.08 and 4.93 (each s, 2 H, C_5H_4), 5.19 (s, 1 H, H^2), 5.37 (s, 2 H, $H^{1,3}$), 6.85, 6.94–7.02, 7.39–7.44 and 7.55–7.57 (each m, 28 H, H^{5-8}, Ph and Sbztz) ppm. $^{31}P\{^1H\}$ NMR (C_6D_6): δ = 54.6 (s, dppf) ppm. IR (KBr): $\tilde{\nu}$ = 3054 (w), 1651 (m), 1541 (m), 1411 (s), 1158 (w, CS), 1089 (m), 1034 (m), 961 (m), 744 (m), 697 (s), 510 (s), 477 (m) cm^{-1}. FAB$^+$-MS: *m*/*z* = 937 $[M]^+$, 822 $[M - Ind]^+$, 771 $[M - Sbztz]^+$, 655 $[M - Ind - Sbztz]^+$. $C_{50}H_{39}FeNP_2RuS_2$ (936.58): calcd. C 64.1, H 4.2, N 1.5, S 6.9; found C 64.4, H 4.1, N 1.3, S 6.6.

[5]Cl: ^{1}H NMR [$(CD_3)_2CO$]: δ = 2.59 (s, 3 H, Me), 4.27, 4.33, 4.42 and 4.67 (each s, 2 H, C_5H_4), 4.84 (s, 2 H, $H^{1,3}$), 5.72 (s, 1 H, H^2), 6.94–7.07, 7.27–7.29, 7.43–7.46 and 7.67–7.76 (each m, 24 H, H^{5-8} and Ph) ppm. $^{31}P\{^1H\}$ NMR [$(CD_3)_2CO$]: δ = 52.9 (s, dppf) ppm. IR (KBr): $\tilde{\nu}$ = 3427 (w, NH), 3052 (w), 2971 (w), 2856 (w), 1479 (w, CS), 1433 (m), 1338 (m), 1155 (w, CS), 1087 (m), 1029 (m), 821 (m), 746 (s), 698 (s), 511 (s) cm^{-1}. FAB$^+$-MS: *m*/*z* = 902 $[M]^+$, 787 $[M - Ind]^+$, 771 $[M - Hmtdzt]^+$. $C_{46}H_{39}ClFeN_2P_2RuS_2$ (938.26): calcd. C 58.9, H 4.2, N 3.0, S 6.9; found C 58.4, H 4.7, N 3.0, S 6.4.

5a: ^{1}H NMR (C_6D_6): δ = 2.27 (s, 3 H, Me), 3.63, 3.85, 4.08 and 4.73 (each s, 2 H, C_5H_4), 5.12 (s, 1 H, H^2), 5.34 (s, 2 H, $H^{1,3}$), 6.97–7.06, 7.10–7.25, 7.42–7.45, 7.53–7.69 and 7.70–7.72 (each m, 24 H, H^{5-8} and Ph), 1.40 and 3.57 (each m, thf) ppm. $^{31}P\{^1H\}$ NMR (C_6D_6): δ = 54.7 (s, dppf) ppm. IR (KBr): $\tilde{\nu}$ = 3059 (w), 2922 (w), 2856 (w), 1648 (m), 1431 (m), 1334 (m), 1157 (m), 1084 (m), 1028 (s), 813 (m), 744 (s), 696 (s), 513 (s) cm^{-1}. FAB$^+$-MS: *m*/*z* = 902 $[M]^+$, 787 $[M - Ind]^+$, 771 $[M - Smtdz]^+$. $C_{46}H_{38}FeN_2P_2RuS_2 \cdot 1.4C_4H_8O$ (1002.61): calcd. C 61.9, H 4.9, N 2.8, S 6.4; found C 62.3, H 5.0, N 3.3, S 6.2.

Reactions of [Ru(CH_3CN)(dppf)(ind)]PF_6 ([2]PF_6)

With HSpym: HSpym (5 mg, 0.04 mmol) was added into a yellow solution of [**2**]PF_6 (28 mg, 0.03 mmol) in thf (8 mL), and the mixture was stirred at room temp. A slow color change to first to orange and then to deep red was observed. After 4 h, the solution was concentrated to ca. 1 mL, and ether (ca. 4 mL) was added. After 1 d at –30 °C, red crystalline solids of [Ru(dppf)(Hpymt)(ind)]PF_6 ([**6**]PF_6) were obtained (15 mg, 50% yield), followed by a second crop (3 mg, 10% yield) upon further concentration of the mother liquor, addition of ether, and similar cooling.

With HSbztz: HSbztz (7 mg, 0.04 mmol) was added into a stirred yellow solution of [**2**]PF_6 (26 mg, 0.03 mmol) in thf (8 mL). The mixture immediately turned reddish-orange, followed by precipitation of crystalline red solids. After 4 h at room temp., the suspension was filtered to afford red crystals of [Ru(dppf)(Hbztzt)(ind)]PF_6 ([**7**]PF_6) (22 mg, 75% yield).

With HSmtdz: HSmtdz (8.5 mg, 0.06 mmol) was added into a yellow solution of [**2**]PF_6 (50 mg, 0.05 mmol) in thf (10 mL), and the mixture was stirred at room temp. The yellow solution slowly turned reddish-orange, accompanied by precipitation of red solids. After 4 h, the red crystalline solids of [Ru(dppf)(Hmtdzt)(ind)]PF_6 ([**5**]PF_6) were filtered and washed with thf (2 × 0.5 mL) and dried (35 mg, 64% yield). A second crop (10 mg, 18% yield) was obtained upon concentration of the mother liquor to ca. 1 mL and addition of hexane (ca. 1 mL). The red solids were recrystallized from CH_2Cl_2/ether to give elementally pure [**5**]PF_6.

Data

[5]PF_6: ^{1}H NMR [$(CD_3)_2CO$]: δ = 2.60 (s, 3 H, Me), 4.22, 4.31, 4.36 and 4.40 (each s, 2 H, C_5H_4), 4.73 (s, 2 H, $H^{1,3}$), 5.66 (s, 1 H, H^2), 6.97–7.03, 7.23–7.28, 7.34–7.42 and 7.60–7.68 (each m, 24 H, H^{5-8} and Ph), 5.63 (CH_2Cl_2) ppm. $^{31}P\{^1H\}$ NMR [$(CD_3)_2CO$]: δ = 54.0 (s, dppf), –142.7 (sept, PF_6) ppm. IR (KBr): $\tilde{\nu}$ = 3310 (w, NH), 3059 (w), 1434 (w, CS), 1159 (w, CS), 1067 (w), 842 (vs, PF_6), 748 (m), 698 (m), 556 (m, PF_6), 510 (m) cm^{-1}. ESI$^+$-MS: *m*/*z* = 903 $[M]^+$, 771 $[M - Hmtdzt]^+$. ESI$^-$-MS: *m*/*z* = 145 $[PF_6]^-$. $C_{46}H_{39}F_6FeN_2P_3RuS_2 \cdot CH_2Cl_2$ (1144.78): calcd. C 49.8, H 3.7, N 2.5, S 5.7; found C 50.0, H 3.5, N 2.5, S 5.8.

[6]PF_6: ^{1}H NMR (C_4D_8O): δ = 2.53 (br., NH), 4.08, 4.22, 4.32 and 4.60 (each s, 2 H, C_5H_4), 4.86 (s, 2 H, $H^{1,3}$), 5.34 (s, 1 H, H^2), 6.91–6.97, 7.06–7.11, 7.18–7.26, 7.52–7.59, 8.31–8.37 (each m, 24 H, H^{5-8} and Ph) ppm. $^{31}P\{^1H\}$ NMR (C_4D_8O): δ = 54.1 (s, dppf), –143.5 (sept, PF_6) ppm. IR (KBr): $\tilde{\nu}$ = 3278 (w, NH), 3055 (w), 1559 (m), 1432 (w, CS), 1374 (m), 1164 (m, CS), 1090 (m), 1035 (m), 844 (vs, PF_6), 698 (m), 553 (m, PF_6), 518 (m) cm^{-1}. ESI$^+$-MS: *m*/*z* = 883 $[M]^+$, 769 $[M - Ind]^+$. ESI$^-$-MS: *m*/*z* = 145 $[PF_6]^-$. $C_{47}H_{39}F_6FeN_2P_3RuS$ (1027.73): calcd. C 54.9, H 3.8, N 2.7, S 3.1; found C 54.5, H 3.5, N 2.7, S 2.9.

[7]PF_6: ^{1}H NMR [$(CD_3)_2CO$]: δ = 4.22, 4.32, 4.40 and 4.56 (each s, 2 H, C_5H_4), 4.78 (s, 2 H, $H^{1,3}$), 5.65 (s, 1 H, H^2), 7.96–7.02 (m, 4 H, Ph and NH), 7.11–7.16, 7.24–7.27, 7.49–7.54, 7.59–7.68 and 7.79–7.82 (each m, 21 H, Ph), 7.29–7.32 and 7.38–7.42 (each m, 4 H, H^{5-8}) ppm. $^{31}P\{^1H\}$ NMR [$(CD_3)_2CO$]: δ = 53.9 (s, dppf), –142.7 (sept, PF_6) ppm. IR (KBr): $\tilde{\nu}$ = 3309 (w, NH), 3058 (w), 2922 (w), 1432 (m, CS), 1326 (w), 1260 (w), 1158 (w, CS), 1087 (m), 1038 (m), 842 (vs, PF_6), 745 (m), 698 (m), 556 (m, PF_6), 509 (m) cm^{-1}. FAB$^+$-MS: *m*/*z* = 938 $[M + H]^+$, 822 $[M - Ind]^+$, 771 $[M - Hbztzt]^+$. FAB$^-$-MS: *m*/*z* = 145 $[PF_6]^-$. $C_{50}H_{40}F_6FeNP_3RuS_2$ (1082.82): calcd. C 55.5, H 3.7, N 1.3, S 5.9; found C 55.2, H 3.5, N 1.3, S 5.8.

Crystal Structure Determinations

Crystals were mounted on quartz fibers. X-ray data were collected with a Bruker AXS APEX system, by using Mo-K_α radiation, with the SMART suite of programs.[18] Data were processed and corrected for Lorentz and polarization effects with SAINT,[19] and for absorption effects with SADABS.[20] Structural solution and refinement were carried out with the SHELXTL suite of programs.[21] Crystal and structure refinement data are summarized in Table 2. The structures were solved by direct methods or Patterson maps to locate the heavy atoms, followed by difference maps for the light, non-hydrogen atoms. All non-hydrogen atoms were generally given anisotropic displacement parameters in the final model.

CCDC-655368 and -655369, for **4** and [**5**]Cl, respectively, contain the supplementary crystallographic data for this paper. These data can be obtained free of charge from The Cambridge Crystallographic Data Centre via www.ccdc.cam.ac.uk/data_request/cif.

Acknowledgments

The authors acknowledge with thanks support from National University of Singapore Academic Research Fund (grant no. 143-000-209-112) to L. Y. G., the Institute of Chemical and Engineering Sciences for research scholarship to S. Y. N., technical assistance from Dr. L. L. Koh and Ms G. K. Tan for X-ray structure determinations, and support from Nanyang Technological University to L. Y. G. and R. D. W.

[1] a) L. Breydo, H. Zang, K. Mitra, K. S. Gates, *J. Am. Chem. Soc.* **2001**, *123*, 2060–2061; b) N. L. Kelleher, C. L. Hendrickson, C. T. Walsh, *Biochemistry* **1999**, *38*, 15623–15630; c) P. W. Baures, *Org. Lett.* **1999**, *1*, 249–252; d) W. C. Groutas, R. Z.

Kuang, S. M. Ruan, J. B. Epp, R. Venkataraman, T. M. Truong, *Bioorg. Med. Chem.* **1998**, *6*, 661–671; e) M. Thomas, D. Guillaume, J.-L. Fourrey, P. Clivio, *J. Am. Chem. Soc.* **2002**, *124*, 2400–2401 and references cited therein; f) T. Kataoka, F. Ohhashi, *Cancer Res.* **1985**, *45*, 2962–2966; g) J. P. Street, K. I. Skorey, R. S. Brown, R. G. Ball, *J. Am. Chem. Soc.* **1985**, *107*, 7669–7679.

[2] a) E. S. Raper, *Coord. Chem. Rev.* **1985**, *61*, 115–184 and references cited therein; E. S. Raper, *Coord. Chem. Rev.* **1996**, *153*, 199–255; E. S. Raper, *Coord. Chem. Rev.* **1997**, *165*, 475–567; b) A. Massey, Y. Z. Xu, P. Karran, *Curr. Biol.* **2001**, *11*, 1142–1146; c) J. Susperregui, M. Bayle, J. M. Léger, G. Délèris, *J. Organomet. Chem.* **1998**, *556*, 105–110; d) N. A. Bell, T. N. Branston, W. Clegg, L. Parker, E. S. Raper, C. Sammon, C. P. Constable, *Inorg. Chim. Acta* **2001**, *319*, 130–136; e) G. Kornis in *1,3,4-Thiadiazoles. Comprehensive Heterocyclic Chemistry* (Eds.: A. R. Katrizky, C. W. Rees), Pergamon Press, Oxford, **1984**, vol. 6, pp. 545.

[3] a) F. Hipler, R. A. Fischer, J. Müller, *J. Chem. Soc. Perkin Trans. 2* **2002**, 1620–1626; b) S. Stoyanov, I. Petkov, L. Antonov, T. Stoyanova, P. Karagiannidis, P. Aslanidis, *Can. J. Chem.* **1990**, *68*, 1482–1489.

[4] M. El-khateeb, *Transition Met. Chem.* **2001**, *26*, 267–270.

[5] S. Y. Ng, G. H. Fang, W. K. Leong, L. Y. Goh, M. V. Garland, *Eur. J. Inorg. Chem.* **2007**, 452–462.

[6] S. Y. Ng, W. K. Leong, L. Y. Goh, R. D. Webster, *Eur. J. Inorg. Chem.* **2007**, 463–471.

[7] S. Y. Ng, W. K. Leong, L. Y. Goh, R. D. Webster, *Eur. J. Inorg. Chem.* **2007**, 3827–3840.

[8] a) A. Giraudeau, L. Ruhlmann, L. El Kahef, M. Gross, *J. Am. Chem. Soc.* **1996**, *118*, 2969–2979; b) K. M. Kadish, N. Guo, E. Van Caemelbecke, A. Froiio, R. Paolesse, D. Monti, P. Tagliatesta, T. Boschi, L. Prodi, F. Bolletta, N. Zaccheroni, *Inorg. Chem.* **1998**, *37*, 2358–2365; c) R. C. Rocha, H. E. Toma, *Can. J. Chem.* **2001**, *79*, 145–156.

[9] a) M. B. Robin, P. Day, *Adv. Inorg. Chem. Radiochem.* **1967**, *10*, 247–422; b) I. D. Moreira, J. B. de Lima, D. W. Franco, *Coord. Chem. Rev.* **2000**, *196*, 197–217; c) W. Kaim, A. Klein, M. Glockle, *Acc. Chem. Res.* **2000**, *33*, 755–763; d) K. D. Demadis, C. M. Hartshorn, T. J. Meyer, *Chem. Rev.* **2001**, *101*, 2655–2685.

[10] X. L. Lu, J. J. Vittal, E. R. T. Tiekink, L. Y. Goh, T. S. A. Hor, *J. Organomet. Chem.* **2004**, *689*, 1444–1451.

[11] a) A. K. Kakkar, N. J. Taylor, T. B. Marder, J. K. Shen, N. Hallinan, F. Basolo, *Inorg. Chim. Acta* **1992**, *198–200*, 219–231, reported for true η^5-coordination: Δ = 0.03 Å; HA = 2.5°; FA = 4.4°; for distorted η^5: Δ = 0.11–0.42 Å; HA = 7–14°; FA = 6–13°; and for true η^3-coordination: Δ = 0.8 Å; FA = 28°. In general, for indenyl complexes considered η^5: $\Delta < 0.25$ Å; HA < 10°; and for those considered η^3: Δ = 0.69–0.80 Å; HA = *ca.* 20–30°; and for those with slight distortion towards η^3: Δ = 0–0.22 Å; HA < 13°. See for instance; b) V. Cadierno, J. Díez, M. P. Gamasa, J. Gimeno, E. Lastra, *Coord. Chem. Rev.* **1999**, *193–195*, 147–205; c) M. J. Calhorda, L. F. Veiros, *Coord. Chem. Rev.* **1999**, *185–186*, 37–51.

[12] C. Landgrafe, W. S. Sheldrick, M. Sudfeld, *Eur. J. Inorg. Chem.* **1998**, 407–414.

[13] a) L. M. Nguyen, M. E. Dellinger, J. T. Lee, R. A. Quinlan, A. L. Rheingold, R. D. Pike, *Inorg. Chim. Acta* **2005**, *358*, 1331–1336; b) N. A. Bell, S. J. Coles, C. P. Constable, D. E. Hibbs, M. B. Hursthouse, R. Mansor, E. S. Raper, C. Sammon, *Inorg. Chim. Acta* **2001**, *323*, 69–77.

[14] a) R. T. Hembre, J. S. McQueen, V. W. Day, *J. Am. Chem. Soc.* **1996**, *118*, 798–803; b) T. Sixt, J. Fiedler, W. Kaim, *Inorg. Chem. Commun.* **2000**, *3*, 80–82.

[15] B. Corain, B. Longato, G. Favero, D. Ajo, G. Pilloni, U. Russo, F. R. Kreissl, *Inorg. Chim. Acta* **1989**, *157*, 259–266.

[16] A. C. Ohs, A. L. Rheingold, M. J. Shaw, C. Nataro, *Organometallics* **2004**, *23*, 4655–4660.

[17] F. Hipler, M. Winter, R. A. Fischer, *J. Mol. Struct.* **2003**, *658*, 179–191.

[18] SMART version 5.628, Bruker AXS Inc., Madison, Wisconsin, USA, **2001**.

[19] SAINT+ version 6.22a, Bruker AXS Inc., Madison, Wisconsin, USA, **2001**.

[20] Sheldrick, G. M. SADABS, **1996**.

[21] SHELXTL version 5.1, Bruker AXS Inc., Madison, Wisconsin, USA, **1997**.

Received: July 25, 2007
Published Online: November 8, 2007

